The assembly of cell-encapsulating microscale hydrogels using acoustic waves

Feng Xu [a], Thomas D. Finley [a], Muge Turkaydin [a], Yuree Sung [a], Umut A. Gurkan [a], Ahmet S. Yavuz [a], Rasim O. Guldiken [b], Utkan Demirci [a,c,*]

[a] Demirci Bio-Acoustic-MEMS in Medicine (BAMM) Laboratory, Center for Biomedical Engineering, Department of Medicine, Brigham and Women's Hospital, Harvard Medical School, Boston, MA, USA
[b] Department of Mechanical Engineering, University of South Florida, Tampa, FL, USA
[c] Harvard-MIT Health Sciences and Technology, Cambridge, MA, USA

ARTICLE INFO

ABSTRACT

Microscale hydrogels find widespread applications in medicine and biology, e.g., as building blocks for tissue engineering and regenerative medicine. In these applications, these microgels are assembled to fabricate large complex 3D constructs. The success of this approach requires non-destructive and high throughput assembly of the microgels. Although various assembly methods have been developed based on modifying interfaces, and using microfluidics, so far, none of the available assembly technologies have shown the ability to assemble microgels using non-invasive fields rapidly within seconds in an efficient way. Acoustics has been widely used in biomedical arena to manipulate droplets, cells and biomolecules. In this study, we developed a simple, non-invasive acoustic assembler for cell-encapsulating microgels with maintained cell viability (>93%). We assessed the assembler for both microbeads (with diameter of 50 μm and 100 μm) and microgels of different sizes and shapes (e.g., cubes, lock-and-key shapes, tetris, saw) in microdroplets (with volume of 10 μL, 20 μL, 40 μL, 80 μL). The microgels were assembled in seconds in a non-invasive manner. These results indicate that the developed acoustic approach could become an enabling biotechnology tool for tissue engineering, regenerative medicine, pharmacology studies and high throughput screening applications.

© 2011 Elsevier Ltd. All rights reserved.

1. Introduction

Hydrogels have attracted increasing interest as intelligent biomaterials with their controllable properties [1–3]. Recently, the convergence of nano and microscale technologies and hydrogels has resulted in the emergence of microscale hydrogels (microgels) with widespread applications [4–6]. For instance, microgels can be used as building blocks for tissue engineering and regenerative medicine [7–10], and as carriers for cell/drug delivery [11,12]. In these applications, directed manipulation of microgels is required to fabricate larger constructs via assembly. Various nano and microscale technologies have been employed to assemble microgels. While manual manipulation provides control over individual microgels [13], it has limited scalability and throughput. Directed assembly approaches, such as programmable molecular recognition and binding scheme [14], hydrophilic—hydrophobic interactions [7], surface template [15], microfluidics [16,17], and magnetic assembly [10], are promising technologies to assemble microgels. Although large gel patterns with controlled features (e.g., shape, size, spatial resolution) have been achieved through directed assembly, there are several challenges associated with these methods including involvement of additional invasive molecules around the gels to facilitate assembly such as cytotoxic organic solvents. These methods also suffer from complexity of the assembly process, long assembly times, and limited throughput. Therefore, there is an unmet need for efficient methods to direct microgel assembly.

It has been possible to manipulate bioparticles (e.g., cells, cell-laden microgels) in microscale volumes to address challenges in medicine [1,18–21]. Acoustics have been traditionally used for medical imaging applications [22–24]. Recently, acoustic techniques, such as ultrasonic standing waves and acoustic droplet based bioprinting [25] have been used as actuation technologies integrated with microfluidics [26–30] to manipulate particles and cells. Examples include particle trapping and aggregation [31–34], continuous-flow-based separation and manipulation of particles and cells [35–39], cell synchronization [40], cell patterning [41], droplet movement, merging, mixing and concentration [42–44], and microcentrifugation [45,46]. Acoustic technologies offer

* Corresponding author. Harvard-MIT Health Sciences and Technology, Cambridge, MA, USA.
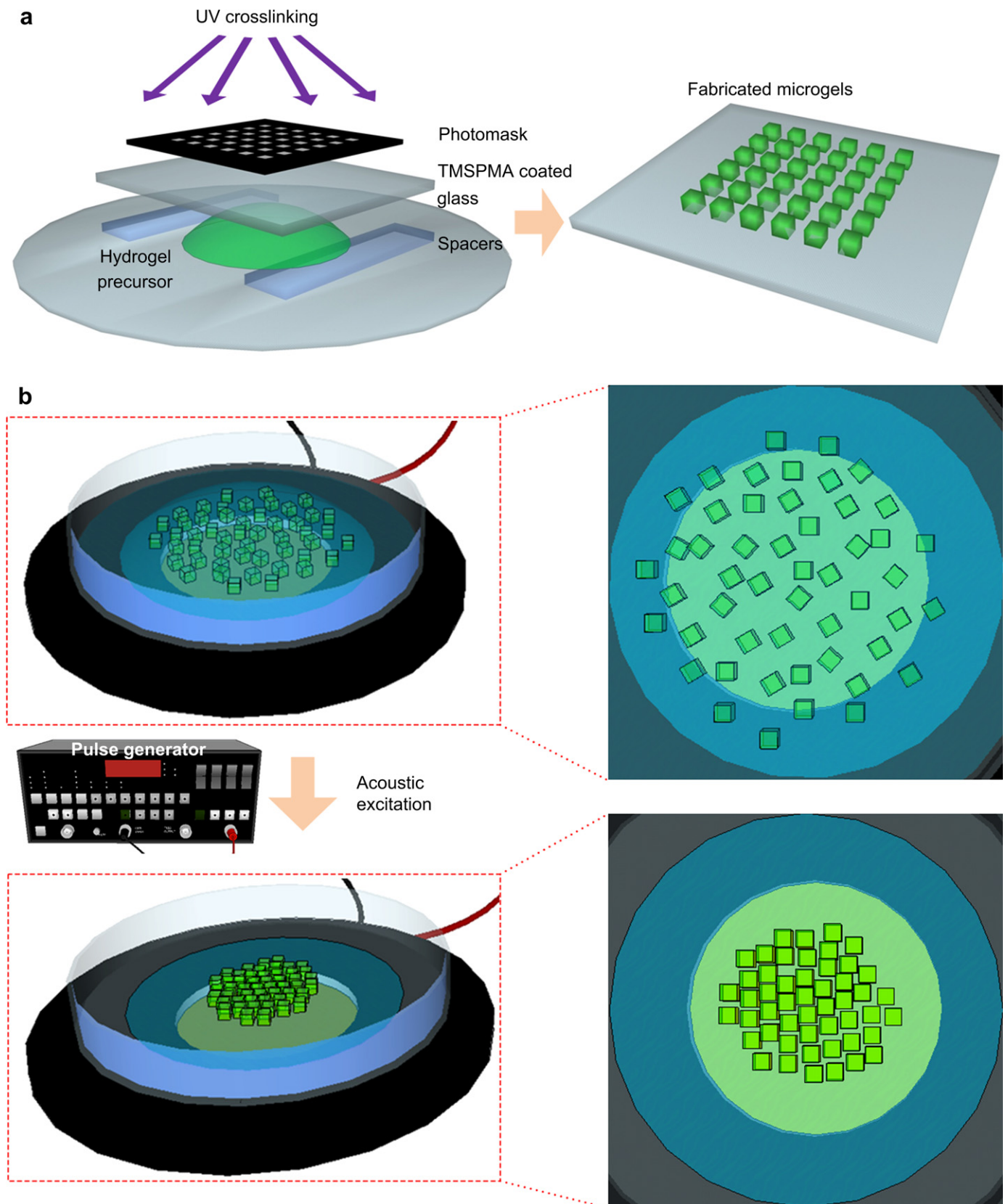E-mail address: udemirci@rics.bwh.harvard.edu (U. Demirci).

Fig. 1. Acoustic microgel assembly process. (a) Fabrication of microgels using photolithography. (b) Assembly of the microgels within a liquid droplet using an acoustic assembler. Distributed microgels were assembled by a transducer during the acoustic excitation.

several advantages such as decreased instrumentation complexity and gentle handling of biological moieties that are sensitive to pressure and heat such as cells and cell-encapsulating microgels, since these techniques are non-invasive [47]. While acoustic technologies have benefited medicine in various areas, they have not yet been utilized for microgel assembly.

In this study, we have developed an acoustic assembler for microgels. A field was applied to a droplet encapsulating microgels of different shapes and sizes to agitate the particles to self-assemble. We assessed the effect of acoustic frequency and amplitude on the assembly process, and the effect of acoustic excitation on the viability of cells encapsulated in the microgels. The acoustic assembly approach is simple, rapid, and cost-effective without need for expensive peripheral equipment, and the assembly is performed in a non-invasive manner without any sample preparation holding great potential for manipulating microgels, particles and cells. Tissues are made of repeating functional units, e.g., the liver is composed of repeating hexagonal lobes, and the pancreas is made up of islets. For instance, microgels encapsulated with cells can be assembled to 3D complex cellular constructs in a high throughput manner, which can be used as a platform for screening cell-drug response, cell–biomaterial interactions.

2. Materials and methods

2.1. Preparation of microgels

Polyethylene glycol (PEG) hydrogel precursor solution was prepared by using 20% (w/w) PEG 1000, 0.05% Irgacure (w/w) and Dulbecco's Modified Eagle Medium (DMEM), Fig. 1a. To fabricate microgels, a droplet of PEG precursor solution (40 μl) was pipetted on the glass slide (25 mm × 25 mm), Fig. 1a. Then, the droplet was covered with a 3-(trimethoxysilyl) propylmethacrylate (TMSPMA) coated glass cover slip and a photomask with a designed shape (square, circular, saw, lock-and-key, and tetris blocks) and size (100–800 μm). The thickness of the microgel was controlled by the changing the number of spacers used (150 μm and 300 μm in this study), Fig. 1a. After 45 s under the UV light (power 2.5 mW/cm^2, height 37 mm), the photomask and glass cover slip were removed and microgels were obtained (Fig. 1a). To render the outside surface of the microgels hydrophilic, the microgels were treated in plasma cleaner (Harrick plasma, Ithaca, NY) for 3 min. The plasma treatment of microgels was performed to enable complete suspension of the microgels in Dulbecco's Phosphate Buffered Saline (DPBS), and hence to prevent the microgels from sticking to the surface of the assembly container (i.e., petri dish surface).

2.2. Preparation of cell-encapsulating microgels

NIH 3T3 mouse fibroblast cells were cultured in DMEM (10% FBS, 1% penicillin-streptomycin) in a standard CO$_2$ incubator (5% CO$_2$). After confluence, the cells were collected through trypsinization and resuspended in the PEG precursor solution at three cell concentrations (1, 5, 10 million cells/mL). The cell-encapsulating microgels were then fabricated following the protocol described above.

2.3. Acoustic assembler

The acoustic assembler was composed of a piezoelectric transducer (Buzzer, CEP 1141, CUI Inc., Tualatin, OR), a frequency generator (HP 8112A), and an assembly chamber (e.g., Petri dish), as depicted in Fig. 1b. The transducer was used to generate acoustic waves, which were transmitted to the particles in the assembly chamber placed above the buzzer top surface. The frequency and intensity of generated acoustic wave were controlled using the pulse generator by varying the pulse frequency (0.8–7.0 kHz) and amplitude (1–16 V) applied to the transducer. The transducer output is maximal at 4.2 kHz as reported in the data sheet.

2.4. Acoustic assembly of microbeads

We used glass beads (Polysciences Inc., Warrington, PA) of two different sizes (i.e., 50 μm, 100 μm in diameter). To assemble the beads, a droplet of DPBS was manually pipetted on the Petri dish (assembly chamber), and the beads were of designed concentration were added into the droplet, Fig. 1b. Then, acoustic wave excitation was applied and the whole assembly process was recorded using a video camera (Sony α700). We quantified the assembly time by analyzing the video using the public domain NIH ImageJ program (developed at the U.S. National Institutes of Health and available at http://rsb.info.nih.gov/nih-image). The assembly time was

defined as when the area change (normalized to initial area) was less than 1%. We assessed the assembly time of beads for four different bead concentrations (i.e., 30 mg/ml, 50 mg/ml, 75 mg/ml, 100 mg/ml), and four droplet volumes (i.e., 10 μL, 20 μL, 40 μL, 80 μL).

2.5. Single-layer assembly of microgels using acoustics

To assemble microgels in a single layer, the microgels were transferred onto a petri dish containing DPBS (Fig. 1b). Acoustic waves were applied at different frequencies and amplitudes to the bottom of the petri dish (Fig. 1b), and the movement of microgels was recorded using a video camera (Sony α700).

2.6. Dual-layer assembly of microgels using acoustic fields

To assemble two layers of microgels, the first layer of microgels were first assembled following the protocol described above. After a single layer was assembled, the construct was stabilized by adding PEG solution (5 μL) followed by a second UV crosslinking. Then, additional microgels were added onto the surface of the assembled first layer. The acoustic assembly process was repeated to build a second layer. The two-layer construct was stabilized by adding PEG solution (5 μL) followed by a second UV crosslinking. The assembled gel construct was then collected by pulling out the droplet.

2.7. Cell viability test

Cell viability was examined using a live/dead assay (Molecular Probes, Invitrogen) and the florescent images were taken using an inverted fluorescent microscope (Nikon, TE2000). Number of living and dead cells were counted using NIH ImageJ program, and cell viability was quantified using the live/dead cell numbers. We quantified cell viability for five sample groups: cells cultured in culture flask (as Control 1), cells suspended in PEG precursor solution before crosslinking (as Control 2), cells encapsulated in PEG microgels after crosslinking, cells encapsulated in PEG microgels after acoustic excitation for 5 s and 30 s. The two time points were chosen based on the duration of acoustic excitation needed to assemble microgels.

3. Results and discussion

We presented a method to acoustically assemble microscale hydrogels encapsulated in a droplet of liquid (Fig. 1). The acoustic directed assembly method conducted in this study manipulated microgels into compact microgel aggregates. To assess the manipulation of particles within the droplets using acoustics, we first studied assembly of 50 μm and 100 μm diameter glass microbeads (Fig. 2). The microbeads were randomly distributed within the droplet before acoustic excitation (Fig. 2a, c). After the acoustic excitation, the beads moved to the center area of the transducer and formed a packed assembly (Fig. 2b, d). To have a quantitative understanding of the interaction of acoustics with particles within the droplets, we also quantified the effect of acoustic frequency, amplitude, droplet size, and bead concentration on the assembly time (Fig. 2e–h). We observed that the frequency (0.8–6.0 kHz) had significant effect on the bead assembly time compared to droplet volume when the bead size and concentration were fixed (Fig. 2e–f). Assembly times decreased significantly with increasing acoustic excitation frequency in the range up to 2 kHz. It didn't change significantly in the range of 2–4 kHz, but increased significantly with further increase in frequency (Fig. 2). For example, for 50 μm beads in droplet volume of 40 μL, the assembly times were 29.30 ± 2.13 (0.8 kHz), 16.02 ± 3.40653 (1 kHz), 3.97 ± 0.87 (1.6 kHz), 2.96 ± 0.32 (2.0 kHz), 3.09 ± 0.09 (3.0 kHz), 4.10 ± 0.17 (3.2 kHz), 1.38 ± 0.19 (4.0 kHz), 2.72 ± 0.60 (4.4 kHz), 8.31 ± 2.43 (5.2 kHz), 34.71 ± 1.58 (6.0 kHz) seconds. Similar trend of frequency-assembly time relationship was also observed for 100 μm beads (Fig. 2f). The observed frequency dependent assembly time can be explained by the transducer used. When the transducer operates close to its resonance (4.2 kHz), it couples more energy hence requires less time to assemble the beads. When the operation frequency is moving away from the resonance, there is less coupling, i.e., longer assembly time. We also checked the assembly time under different excitation amplitudes (0–16 V). We observed that assembly time decreased as the amplitude increased
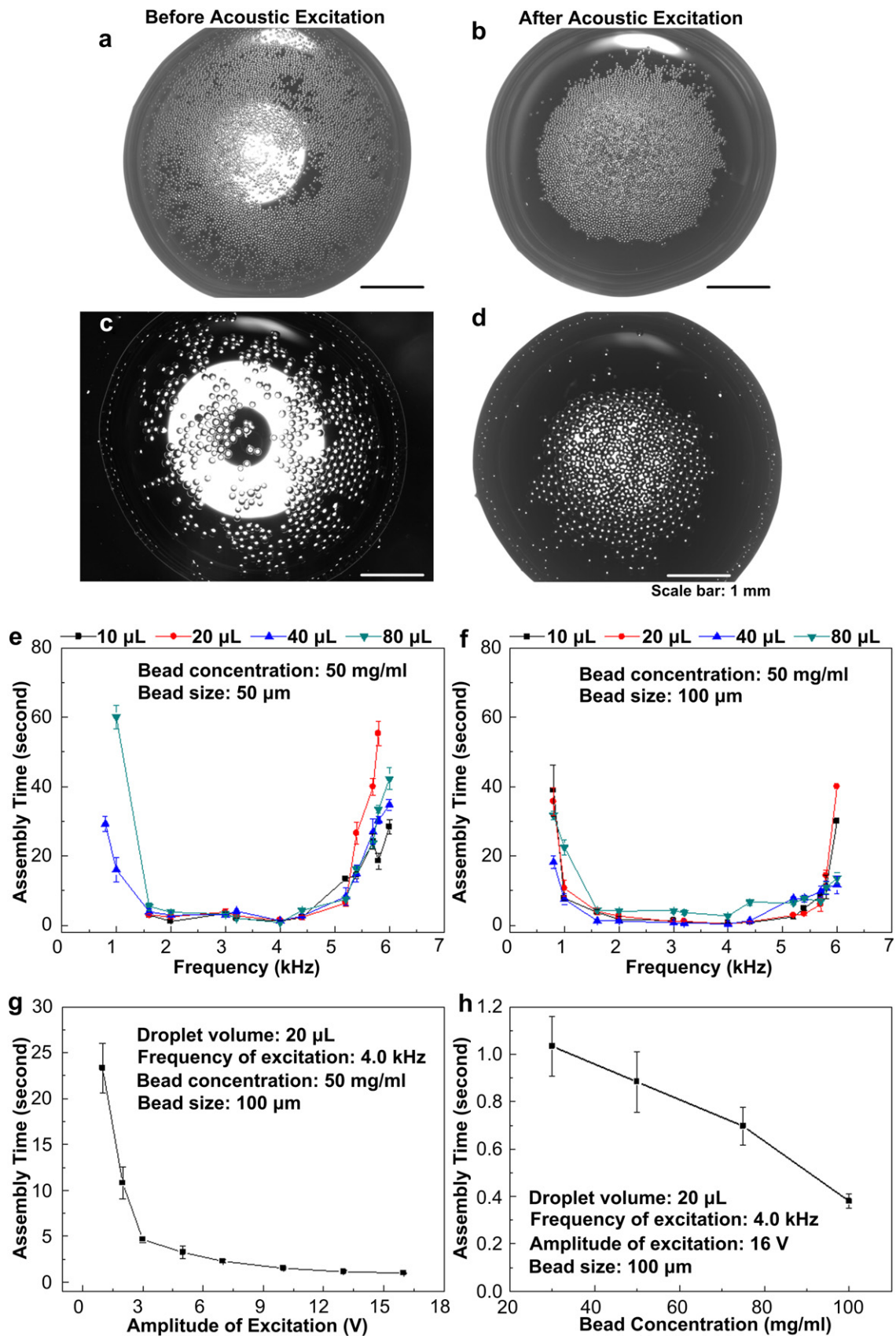
Fig. 2. Acoustic assembly of microbeads. Images of (a) distributed 50 μm microbeads before acoustic excitation, and (b) after acoustic excitation. Bead concentration was 50 mg/mL. Images of (c) distributed 100 μm microbeads before acoustic excitation, and (d) after acoustic excitation. Bead concentration was 50 mg/mL. Assembly time versus frequency for different drop sizes for (e) 50 μm beads and (f) 100 μm beads. (g) Assembly time versus amplitude of excitation for a 20 μL droplet. (h) Assembly time versus bead concentration within a 20 μL droplet.

(Fig. 2g). The assembly times were 23.32 ± 2.70, 10.79 ± 1.73, 4.65 ± 0.33, 3.25 ± 0.65, 2.27 ± 0.22, 1.53 ± 0.12, 1.13 ± 0.15, 0.99 ± 0.06 s for amplitudes of 1, 2, 3, 5, 7, 10, 13, 16 V, respectively. Finally, we observed that the assembly time decreased with increasing bead concentration within the liquid droplet of fixed volume (Fig. 2h). The assembly times were 1.03 ± 0.13, 0.88 ± 0.13, 0.70 ± 0.08, 0.38 ± 0.03 s for bead concentrations of 30, 50, 75, 100 mg/mL, respectively. At higher concentrations, beads need to travel less distance before contacting with another bead since the droplet volume was fixed (20 μL).

To evaluate the ability of the acoustic wave on assembling microgels, we tested several different shapes of microgels (square, lock-and-key, Tetris, saw) to form single-layer assembly, Fig. 3. We first assembled microgels of simple shapes (400 μm square), Fig. 3a. Similar to the microbead assembly, the distributed microgels were placed onto a center area over the transducer and assembled after acoustic excitation was applied (Fig. 3a). We also quantified the microgel assembly process in the form of area change with duration of the acoustic excitation, which was normalized to area before acoustic excitation (Fig. 3b). We observed that the normalized area decreased with duration of

acoustic excitation exponentially, which was 0.98, 0.89, 0.83, 0.81 at $t = 1, 2, 5, 20$ s respectively. We also checked the acoustic assembly of microgels of complex shapes, including lock-and-key (Fig. 3d–e), tetris (Fig. 3b), and saw (Fig. 3g). However, we observed that as the individual shapes and assembly patterns of the microgels were designed to be more complex (e.g., lock-and-key, Tetris, saw), the assembly time increased. For example, the assembly times for the lock-and-key microgels (>60 s) were greatly increased compared to those for microbeads (~1 s) or square microgels (~20 s).

To assess the capability of acoustic method to fabricate complex constructs, we assembled microgels into a two-layer construct, Fig. 4. Distributed microgels (Fig. 4a) were first assembled into single layer using acoustic excitation (Fig. 4 b and e), which was stabilized by secondary crosslinking (Fig. 4c). Additional microgels were then introduced on the surface of the assembled single layer, and the acoustic excitation was applied to form assembled second layer (Fig. 4d and f). Also, the droplets were in a locally humid environment and did not rapidly dry out during assembly. Via this layer–layer approach, a multi-layer construct was fabricated (Fig. 4g).
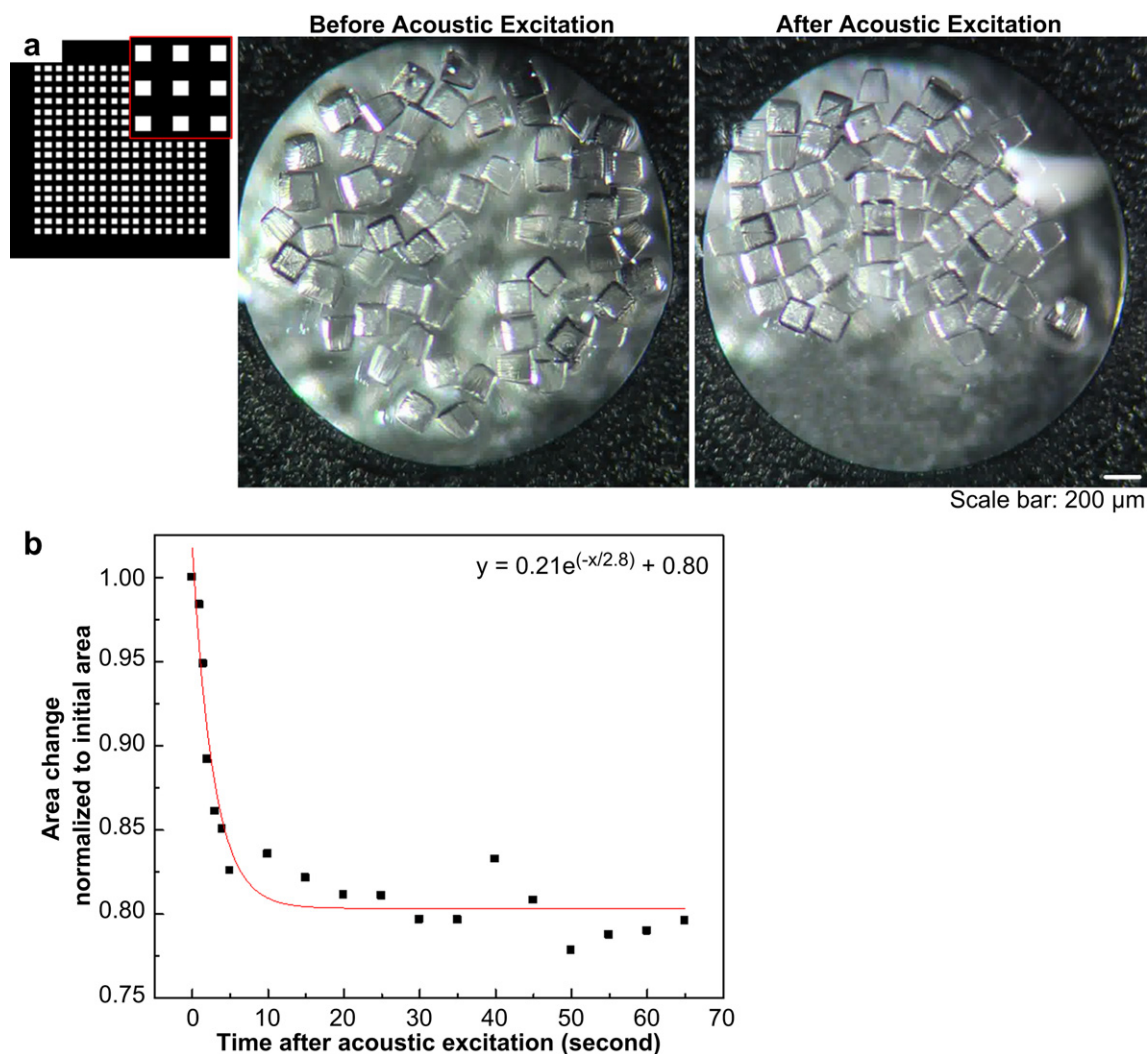

Fig. 3. Single-layer assembly of microgels via acoustic excitation. (a) Images of 200 μm square microgels before and after acoustic excitation. (b) Change of normalized area with duration of the acoustic excitation. (c)–(d) Images of lock-and-key microgels before and after acoustic excitation. Circular microgels (200 μm in diameter) were connected by a star-shaped microgel, while 200 μm circular microgels were enclosed in 1 mm square microgels. (e) Images of Z-shaped tetris blocks before and after acoustic excitation. (f) Images of 1 mm saw-shaped microgels before and after acoustic excitation.
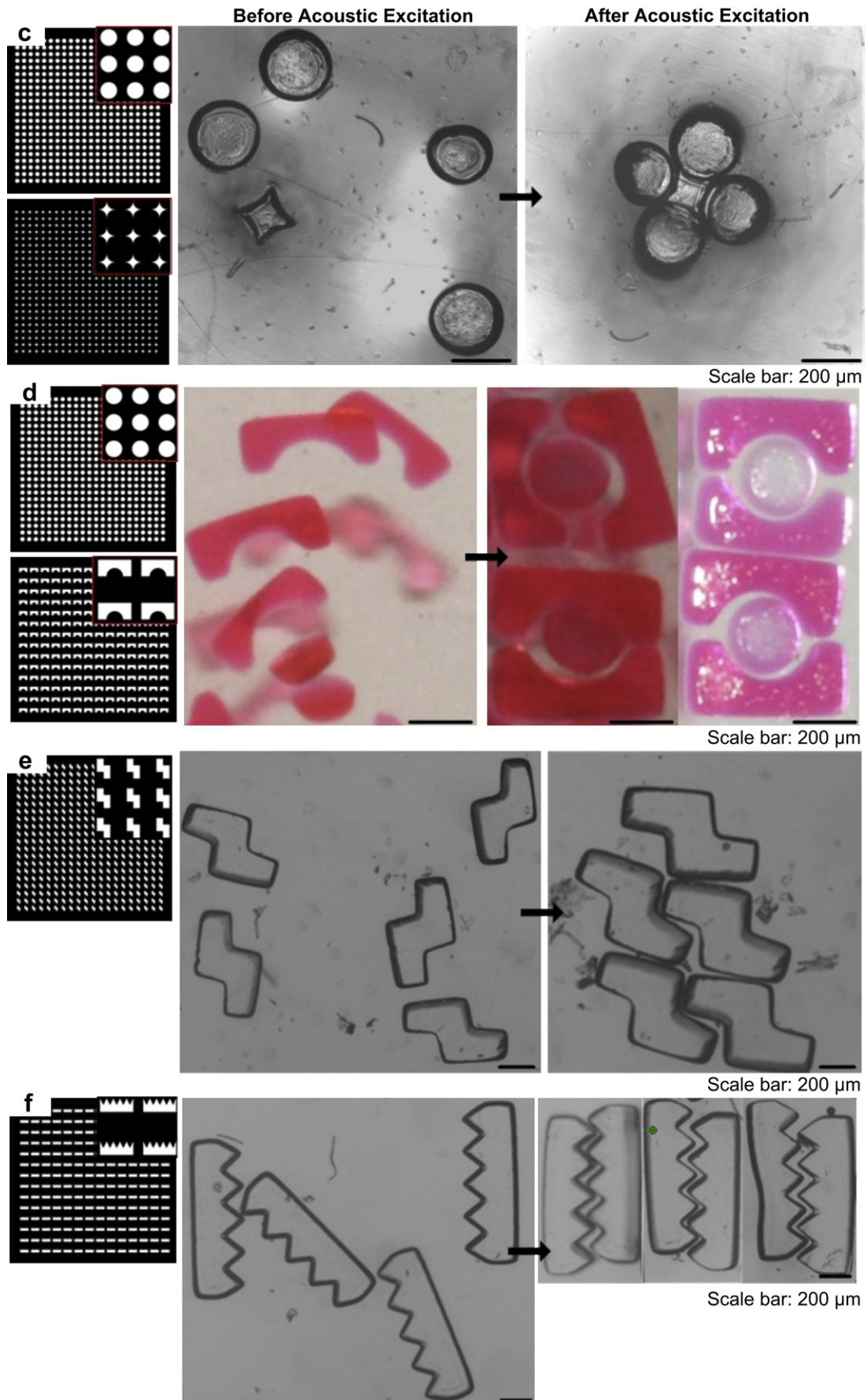
Before Acoustic Excitation **After Acoustic Excitation**

Scale bar: 200 μm

Scale bar: 200 μm

Scale bar: 200 μm

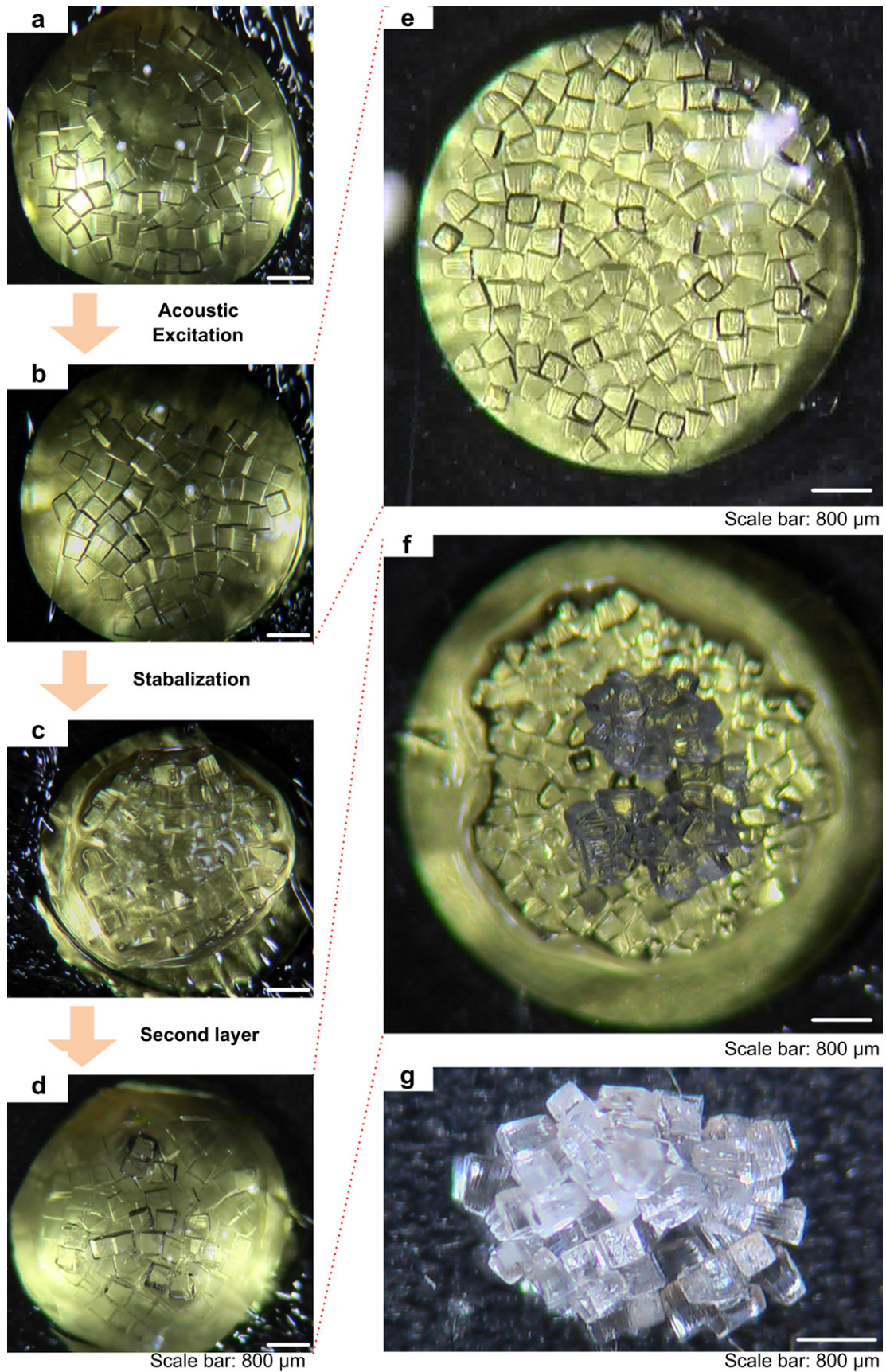Scale bar: 200 μm

Fig. 3. (continued).

Fig. 4. Multi-layer assembly of microgels via acoustics. (a) Distributed microgels were first assembled into (b) single layer using acoustic excitation. (c) The single-layer assembly was stabilized by second crosslinking. (d) New microgels were then introduced on the surface of the assembled single layer to form assembled second layer. (e) Enlarged image of single-layer assembly. (f) Enlarged image of double-layer assembly. (g) Image of fabricated multi-layer hydrogel construct.
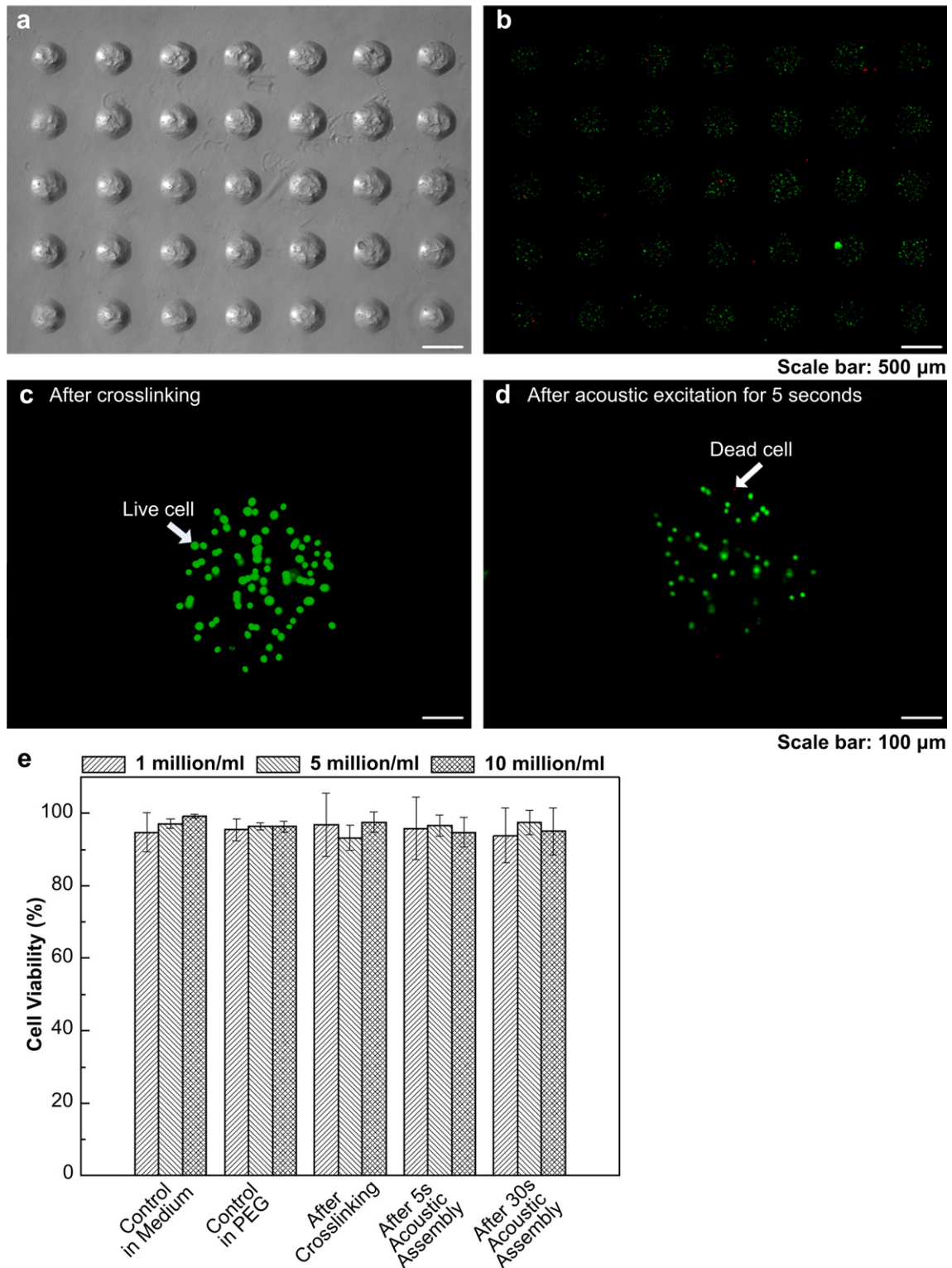
Fig. 5. Viability of cells encapsulated in microgels during the acoustic assembly process. (a) Fabricated cell-encapsulating microgels and (b) corresponding fluorescent images of live/dead staining after crosslinking. Cell viability in individual microgels after (c) crosslinking and (d) after acoustic excitation for 5 s. (e) Quantification of cell viability in medium, in PEG, after crosslinking and after acoustic excitation (5 s and 30 s).

To check the effect of acoustic excitation process on cells encapsulated in the microgels, we evaluated cell viability of fibro-blasts at three cell concentrations (1, 5, 10 million cells/mL), Fig. 5. Cells were encapsulated in microgels using photolithography (Fig. 5a). We observed that cells remained viable after crosslinking (Fig. 5b–c) and acoustic excitation (Fig. 5d), and there were only few dead cells. For cell concentration of 5 million cells/mL, cell viability percentage was 97.2 ± 1.2 in medium, 96.4 ± 1.0 in hydrogel precursor solution, 93.2 ± 3.4 after crosslinking, 96.6 ± 2.9 and 97.5 ± 3.3 after acoustic excitation for 5 s and 30 s

respectively (Fig. 5e). These results indicated that crosslinking and acoustic excitation didn't have significant effect on cell viability compared to controls.

4. Conclusion

In summary, we demonstrated a method of acoustic directed assembly of cell-encapsulating microgels in a rapid, non-invasive manner. The acoustic assembly method presented here can be used to fabricate multi-layer constructs via a layer-by-layer approach. Therefore, the acoustic assembly approach can become an enabling biotechnology tool for applications in the field of tissue engineering and regenerative medicine, pharmacological studies, and high throughput screening applications.

Author contributions

U.D. suggested the idea and F.X. and U.D. designed the research; T.D.F., M.T., Y.S., A.S.Y., and U.A.G. performed research; F.X., T.D.F., M.T., and R.G. analyzed data; F.X., T.D.F., and U.D. wrote the paper.

Acknowledgments

References

[1] Geckil H, Xu F, Zhang X, Moon S, Demirci U. Engineering hydrogels as extra-cellular matrix mimics. Nanomedicine (Lond) 2010;5:469–84.

[2] Jay SM, Saltzman WM. Shining light on a new class of hydrogels. Nat Biotechnol 2009;27:543–4.

[3] Slaughter BV, Khurshid SS, Fisher OZ, Khademhosseini A, Peppas NA. Hydrogels in regenerative medicine. Adv Mater 2009;21:3307–29.

[4] Saunders BR, Laajam N, Daly E, Teow S, Hu X, Stepto R. Microgels: from responsive polymer colloids to biomaterials. Adv Colloid Interface Sci 2008; 147–148:251–62.

[5] Seiffert S, Thiele J, Abate AR, Weitz DA. Smart microgel capsules from macromolecular precursors. J Am Chem Soc 2010;132:6606–9.

[6] Xu F, Wu JH, Wang SQ, Durmus NG, Gurkan UA, Demirci U. Microengineering methods for cell-based arrays and their application in high throughput drug screening. Biofabrication, in press.

[7] Du Y, Lo E, Ali S, Khademhosseini A. Directed assembly of cell-laden microgels for fabrication of 3D tissue constructs. Proc Natl Acad Sci U S A 2008;105:9522–7.

[8] Moon S, Hasan SK, Song YS, Xu F, Keles HO, Manzur F, et al. Layer by layer three-dimensional tissue epitaxy by cell-laden hydrogel droplets. Tissue Eng Part C Methods 2010;16:157–66.

[9] Xu F, Moon SJ, Emre AE, Turali ES, Song YS, Hacking SA, et al. A droplet-based building block approach for bladder smooth muscle cell (SMC) proliferation. Biofabrication 2010;2:014105.

[10] Xu F, Wu C-aM, Rengarajan V, Finley TD, Keles HO, Sung Y, et al. Three-dimensional magnetic assembly of microscale hydrogels. Adv Mater, in press.

[11] Rabanel JM, Banquy X, Zouaoui H, Mokhtar M, Hildgen P. Progress technology in microencapsulation methods for cell therapy. Biotechnol Prog 2009;25: 946–63.

[12] Oh JK, Drumright R, Siegwart DJ, Matyjaszewski K. The development of microgels/nanogels for drug delivery applications. Prog Polym Sci 2008;33:448–77.

[13] Yeh J, Ling Y, Karp JM, Gantz J, Chandawarkar A, Eng G, et al. Micromolding of shape-controlled, harvestable cell-laden hydrogels. Biomaterials 2006;27: 5391–8.

[14] Sacanna S, Irvine WT, Chaikin PM, Pine DJ. Lock and key colloids. Nature 2010; 464:575–8.

[15] Du Y, Ghodousi M, Lo E, Vidula MK, Emiroglu O, Khademhosseini A. Surface-directed assembly of cell-laden microgels. Biotechnol Bioeng 2010;105:655–62.

[16] Chung SE, Park W, Shin S, Lee SA, Kwon S. Guided and fluidic self-assembly of microstructures using railed microfluidic channels. Nat Mater 2008;7:581–7.

[17] Cheung YK, Gillette BM, Zhong M, Ramcharan S, Sia SK. Direct patterning of composite biocompatible microstructures using microfluidics. Lab Chip 2007; 7:574–9.

[18] Song YS, Lin RL, Montesano G, Durmus NG, Lee G, Yoo SS, et al. Engineered 3D tissue models for cell-laden microfluidic channels. Anal Bioanal Chem 2009; 395:185–93.

[19] Song YS, Adler D, Xu F, Kayaalp E, Nureddin A, Anchan RM, et al. Vitrification and levitation of a liquid droplet on liquid nitrogen. Proc Natl Acad Sci U S A 2010;107:4596–600.

[20] Samot J, Moon S, Shao L, Zhang X, Xu F, Song Y, et al. Blood banking in living droplets. PLoS One 2011;6:e17530.

[21] Moon S, Kim YG, Dong L, Lombardi M, Haeggstrom E, Jensen RV, et al. Drop-on-demand single cell isolation and total RNA analysis. PLoS One 2011;6: e17455.

[22] Johnson JA, Oralkan O, Ergun S, Demirci U, Karaman M, Khuri-Yakub BT. Coherent array imaging using phased subarrays. Part II: simulations and experimental results. IEEE Trans Ultrason Ferroelectr Freq Control 2005;52: 51–64.

[23] Johnson J, Oralkan O, Demirci U, Ergun S, Karaman M, Khuri-Yakub P. Medical imaging using capacitive micromachined ultrasonic transducer arrays. Ultrasonics 2002;40:471–6.

[24] Demirci U, Ergun AS, Oralkan O, Karaman M, Khuri-Yakub BT. Forward-viewing CMUT arrays for medical imaging. IEEE Trans Ultrason Ferroelectr Freq Control 2004;51:887–95.

[25] Tasoglu S, Kaynak G, Szeri AJ, Demirci U, Muradoglu M. Impact of a compound droplet on a flat surface: a model for single cell epitaxy. Phys Fluids 2010;22: 082103.

[26] Laurell T, Petersson F, Nilsson A. Chip integrated strategies for acoustic separation and manipulation of cells and particles. Chem Soc Rev 2007;36: 492–506.

[27] Nilsson J, Evander M, Hammarstrom B, Laurell T. Review of cell and particle trapping in microfluidic systems. Anal Chim Acta 2009;649:141–57.

[28] Demirci U, Montesano G. Single cell epitaxy by acoustic picolitre droplets. Lab Chip 2007;7:1139–45.

[29] Demirci U, Montesano G. Cell encapsulating droplet vitrification. Lab Chip 2007;7:1428–33.

[30] Demirci U. Acousitc picoliter droplets for emerging application in semiconductor industry and biotechnology. J Microelectromech S 2006;15:11.

[31] Shi J, Mao X, Ahmed D, Colletti A, Huang TJ. Focusing microparticles in a microfluidic channel with standing surface acoustic waves (SSAW). Lab Chip 2008;8:221–3.

[32] Svennebring J, Manneberg O, Skafte-Pedersen P, Bruus H, Wiklund M. Selective bioparticle retention and characterization in a chip-integrated confocal ultrasonic cavity. Biotechnol Bioeng 2009;103:323–8.

[33] Manneberg O, Vanherberghen B, Svennebring J, Hertz HM, Onfelt B, Wiklund M. A three-dimensional ultrasonic cage for characterization of individual cells. Appl Phys Lett 2008;93:063901–3.

[34] Raghavan RV, Friend JR, Yeo LY. Particle concentration via acoustically driven microcentrifugation: microPIV flow visualization and numerical modelling studies. Microfluidics and Nanofluidics 2010;8:73–84.

[35] Renaudin A, Tabourier P, Zhang V, Camart JC, Druon C. SAW nanopump for handling droplets in view of biological applications. Sensors Actuators B Chem 2006;113:389–97.

[36] Persson J, Augustsson P, Laurell T, Ohlin M. Acoustic microfluidic chip technology to facilitate automation of phage display selection. FEBS J 2008;275: 5657–66.

[37] Franke T, Braunmuller S, Schmid L, Wixforth A, Weitz DA. Surface acoustic wave actuated cell sorting (SAWACS). Lab Chip 2010;10:789–94.

[38] Petersson F, Aberg L, Sward-Nilsson AM, Laurell T. Free flow acoustophoresis: microfluidic-based mode of particle and cell separation. Anal Chem 2007;79: 5117–23.

[39] Shi J, Huang H, Stratton Z, Huang Y, Huang TJ. Continuous particle separation in a microfluidic channel via standing surface acoustic waves (SSAW). Lab Chip 2009;9:3354–9.

[40] Thevoz P, Adams JD, Shea H, Bruus H, Soh HT. Acoustophoretic synchronization of mammalian cells in microchannels. Anal Chem 2010;82:3094–8.

[41] Shi J, Ahmed D, Mao X, Lin SC, Lawit A, Huang TJ. Acoustic tweezers: patterning cells and microparticles using standing surface acoustic waves (SSAW). Lab Chip 2009;9:2890–5.

[42] Bourquin Y, Reboud J, Wilson R, Cooper JM. Tuneable surface acoustic waves for fluid and particle manipulations on disposable chips. Lab Chip 2010;10: 1898–901.

[43] Wixforth A. Acoustically driven planar microfluidics. Superlattice Microst 2003;33:389–96.

[44] Tan MK, Friend JR, Yeo LY. Microparticle collection and concentration via a miniature surface acoustic wave device. Lab Chip 2007;7:618–25.

[45] Li H, Friend JR, Yeo LY. Surface acoustic wave concentration of particle and bioparticle suspensions. Biomed Microdevices 2007;9:647–56.

[46] Yeo LY, Friend JR. Ultrafast microfluidics using surface acoustic waves. Biomicrofluidics 2009;3:012002–23.

[47] Foster FS, Pavlin CJ, Harasiewicz KA, Christopher DA, Turnbull DH. Advances in ultrasound biomicroscopy. Ultrasound Med Biol 2000;26:1–27.